Absence of surface states for LiFeAs investigated using density functional calculations

Alexander Lankau, Klaus Koepernik, Sergey Borisenko, Volodymyr Zabolotnyy, Bernd Büchner, Jeroen van den Brink, and Helmut Eschrig*
IFW Dresden, P.O. Box 270116, D-01171 Dresden, Germany
(Received 7 July 2010; revised manuscript received 31 August 2010; published 10 November 2010)

We investigate the cleaving behavior of LiFeAs and determine its surface electronic structure by detailed density functional calculations. We show that due to the neutral surface of LiFeAs after cleaving, barely any influence of the surface on the electronic states is present. Therefore the data of surface sensitive probes such as angle-resolved photoemission spectroscopy (ARPES) represent to a high degree the bulk electronic structure. This we highlighted by a direct comparison of the calculations to ARPES spectra.

DOI: 10.1103/PhysRevB.82.184518 PACS number(s): 68.35.bd, 74.20.Pq, 74.25.Jb, 74.70.Xa

The use of angle-resolved photoemission (ARPES) and scanning tunneling spectroscopies to study the electronic structure of iron pnictides can turn out to be crucial to understand the superconductivity in these materials. On one hand, both methods are very informative by providing the detailed distribution of electron density in real and reciprocal spaces but on the other hand it is not clear whether the obtained information is related to the bulk or surface.

In a recent paper[1] we found a pronounced surface electronic structure in LaOFeAs, which appears to be present in published ARPES data.[2–7] LaOFeAs single crystals cleave between the La and As layers forming a polar surface. In contrast LiFeAs, of which clean large single crystals are now available,[8–10] can be expected to cleave between adjacent Li layers and hence to produce a neutral surface. This is confirmed by results of density-functional-theory (DFT) calculations presented below.

Although LiFeAs in bulk is found much more three-dimensional (3D) compared to LaOFeAs in DFT calculations,[11–13] its surface electronic structure is much more bulklike. Surface sensitive probes are therefore expected to directly yield information on the bulk behavior. Also, undoped stoichiometric LiFeAs is superconducting below 18 K and does not order magnetically.[10,14]

Recent ARPES experiments on LiFeAs have revealed several interesting features. Although the low-energy electronic structure is qualitatively similar to other Fe pnictides, the Fermi surface of LiFeAs is remarkably different. It shows a strongly reduced tendency to (π,π) nesting,[15] which is present in most of the new iron superconductors and often believed to be characteristic for all of them. As shown in Fig. 5, the radii of the hole and electron cylinders are quite different here. Another observation is the renormalization of the conduction bands by a factor up to 3 as compared to DFT calculations with an extended van Hove singularity (flat maximum of the h_2 band) in the center of the Brillouin zone (BZ). The four bands supporting the Fermi surface were found to be differently, though isotropically, gapped in the superconducting state.[15] These observations can have important implications for understanding the mechanism of superconductivity in the Fe pnictides. Here we show that there is no surface driven electronic structure in LiFeAs and therefore surface sensitive measurements represent the bulk electronic structure as opposed to the situation in the 1111 (e.g., LaOFeAs) compounds.

Non-spin-polarized scalar relativistic DFT total energy and Kohn-Sham band-structure calculations were performed with the full-potential local-orbital code version FPLO9.00.[16] All considered structures were fully relaxed with the generalized-gradient-approximation (GGA) functional[17] using the force tool of FPLO9.00. Forces were minimized to less then 5×10^{-3} eV/Å for bulk and 10^{-1} eV/Å for slab calculations. This is necessary since no detailed surface structure is known from experiment.

The calculations were carefully converged with the number of k points, and finally $12\times12\times4$, regular k-point meshes were used in the full BZ. The densities were converged down to 10^{-6} for the corresponding parameter in FPLO $[\mathrm{rms}(\rho^{\mathrm{out}}-\rho^{\mathrm{in}})/\mathrm{uc}]$. Table I shows the results for the bulk lattice parameters compared to experiment.[10,14,18]

One can observe a decrease in volume of the cell, compared to experimental data, which is reflected in a c-lattice-parameter reduction due to the softness of the lattice in z direction (cf. LaOFeAs in Ref. 1). This slight underestimation of the lattice parameters even in GGA calculations is a common feature for non-spin-polarized calculations in the pnictide family due to the strong coupling of magnetism to the lattice. However, the differences remain acceptable although the deviation for the distance in z direction between adjacent Fe and As layers $d_{\mathrm{Fe\text{-}As}}$ is approximately 3%. The local-density approximation, would result in even further reduced a and c values (results not shown) hence GGA was used throughout this work.

After relaxation, the next step was to calculate the cleaving behavior of LiFeAs by the same approach as in Ref. 1. We had to use an orthorhombic $Pmm2$ space group instead of $P4/nmm$, in order to allow all atom layers to relax in z direction, unconstrained by symmetry.

In order to study the cleaving behavior we constructed a supercell with two unit cells in z direction with lattice constant $2c$. For $c=c_{\mathrm{bulk}}$ this just represents a bulk calculation. Now, we apply tensile strain in z direction, by increasing c. We performed a set of calculations for c values, which correspond to 0%, 10%, 20%, and 30% strain.

Figure 1 shows the inter and intra-unit-cell layer distances of different atomic layers, such as Li-Li (straight and dashed lines), Fe-As (dotted line), and Li-As (dashed-dotted line) for this periodic superstructure of two unit cells in z direction as a function of tensile strain. At large enough strain the original periodicity of period c in z direction is broken by forming

TABLE I. Structure parameters of bulk LiFeAs; $d_{\text{Fe-As}}$ is the atom layer distance in z direction; experimental data taken from Ref. 14.

	a (Å)	c (Å)	z_{As}	z_{Li}	$d_{\text{Fe-As}}$ (Å)
Experiment	3.791	6.364	0.2635	0.8459	2.420
GGA	3.766	6.158	0.2729	0.8325	2.345

slits. By our adopted superstructure of two unit cells, slits form between every other Li-Li layer pair. (*Inter* indicates the distance crossing the slit, when it is formed while *intra* corresponds to distances within the two unit-cell slab [Li|As|Fe_2|As|Li|Li|As|Fe_2|As|Li].)

For small strain the whole slab is more or less uniformly stretched with all the layer distances increasing compared to their bulk values. From the calculated forces of about 0.2 eV/Å one infers a tensile stress in z direction of 2.1 GPa for 10% tensile strain. For a strain between 10% and 20%, LiFeAs cleaves between two Li layers in our calculations with a resulting neutral surface and consequently a nonpolar slab, as we pointed out above (see also Ref. 15). Cleavage here means that the layers are no longer uniformly stretched but that the two unit cells relax back to bulklike distances while a slit (vacuum) opens up between two Li layers such that we have a repeated slab setup with a slab thickness of two unit cells. In the doubled unit cell the interior Li-Li layer distance (termed *intracell* in Fig. 1) relaxes back even below the bulk value. Also the topmost Li-As layer distance close to the slit reduces appreciably while the Fe-As layer distance hardly changes. (It should be pointed out that our simulation of the cleaving process only provides its qualitative behavior because the chosen supercell may not be large enough to simulate true bulklike behavior in the interior layers.)

To obtain a reliable lattice and electronic structure of a cleaved crystal surface it is necessary to choose a slab that is thick enough to pin the Fermi level of the slab to the bulk

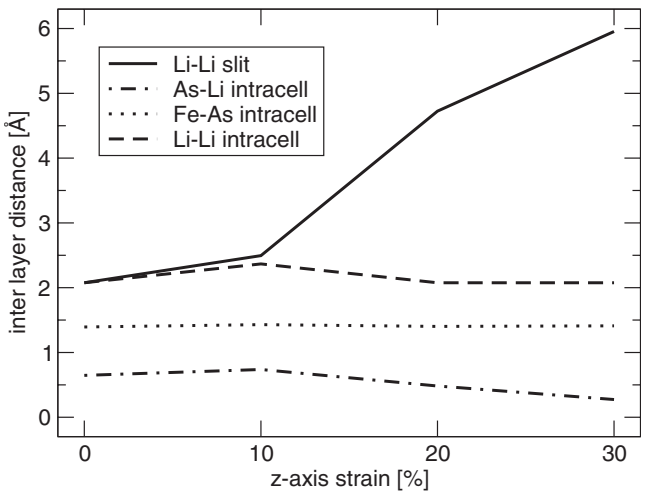

FIG. 1. Interlayer distances of LiFeAs as a function of tensile strain in z direction. The lines between data points are guides for the eye.

TABLE II. Upper part: interlayer distances in Å. Lower part: electron excess per site. Left and right double column: see explanation in the text. In view of the mirror symmetry with respect to the central layer only half of a slab is represented.

	Bulk (4*uc*)	3/1 slab	3/3 slab	Bulk (6*uc*)
...	...	Vac.	Vac.	...
Li/As	0.650	0.496	0.498	0.650
As/Fe	1.398	1.425	1.424	1.398
Fe/As	1.398	1.396	1.396	1.398
As/Li	0.650	0.634	0.636	0.650
Li/Li	2.062	2.065	2.066	2.062
Li/As	0.650	0.643	0.644	0.650
As/Fe	1.398	1.398	1.399	1.398
...	...	...	...	...
...	...	Vac.	Vac.	...
Li	−0.144	−0.161	−0.162	−0.144
As	+0.296	+0.426	+0.426	+0.296
Fe_2	−0.304	−0.375	−0.380	−0.304
As	+0.296	+0.269	+0.267	+0.296
Li	−0.144	−0.155	−0.152	−0.144
Li	−0.144	−0.146	−0.144	−0.144
As	+0.296	+0.295	+0.293	+0.296
Fe_2	−0.304	−0.304	−0.297	−0.304
...	...	...	...	...

value and to choose a slit that is wide enough so that electronic wave functions from both sides of the slit do not overlap. (Due to the chosen mirror symmetry in the center of the slab (z direction) there is no electric field across the slit.) It turns out that the Fermi level of even a slab thickness of only three unit cells hardly changes compared to the bulk, indicating that this thickness is already sufficient. To check convergence with the vacuum layer width, calculations were done with a slit width of about c_{bulk} (resulting in a periodicity $4c$ for the repeated three unit-cells slab; termed 3/1 in Table II) and with a slit width of about $3c$ (resulting in a periodicity of $6c$ for the whole repeated slab setup, termed 3/3). In order to have k-integration errors under control, the bulk calculations (used for comparison in Table II) were done with supercells of the same periodicity in z direction (four and six unit cells, respectively) allowing for the same k-mesh interpolation in both bulk and slab cases. The two different vacuum setups with their corresponding bulk calculations are represented by the left and right double columns in Table II.

When comparing the inner layer distances and layer charges of the slab with those of the bulk crystal (lower parts of both subpanels in Table II), one sees that a slab of three unit cells thickness is already giving bulk representative interior layers. From the residual forces the numerical accuracy of the distances is estimated to be better than 0.01 Å while the accuracy of the layer charges is better than 0.005 of the electron charge. Also the positions and charges between a calculation with a vacuum width of c and $3c$ barely differ so that in what follows the 3/1 slab is used for the surface band-structure analysis.

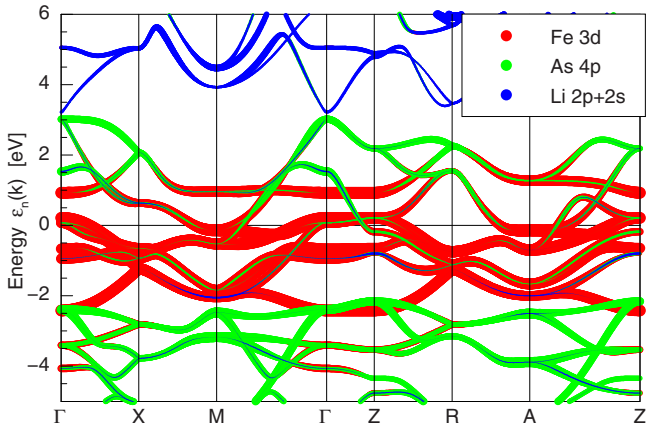

FIG. 2. (Color online) Band structure of bulk LiFeAs, orbital projected onto the leading Fe, As, and Li orbitals.

As is seen from the upper parts of Table II, there is a slight outward shift of the topmost As layer beneath the surface and an appreciable inward shift of the Li surface layer. Interestingly, this causes a charge redistribution between the As layer and the Fe layer below of about 0.1 electron charge but nearly no change in the Li layer charge.

After having justified our model, we will inspect more closely Figs. 2–4, which show results for the band structure and Fermi surface (FS). In Fig. 2 we present the orbital projected band structure for the bulk calculation. The orbital projection is obtained by projecting the Kohn-Sham wave functions onto the chemical orbitals of the FPLO basis. The linewidth of the colored lines in Fig. 2 indicates the orbital content/character in the wave function for every band. As is well known the Fe $3d$ bands (shown in red color or dark gray print) together with some hybridization of the As $4p$ states (green color or light gray print) dominate the entire low-energy spectrum. This is responsible for the metallic behavior of LiFeAs.

However, it is important to note the strong z dispersion of a Li band (shown in blue color or black print), coming from about 5 eV between M and Γ down to Γ (at 3eV) and going further down to −2 eV via several branches along Γ-M and

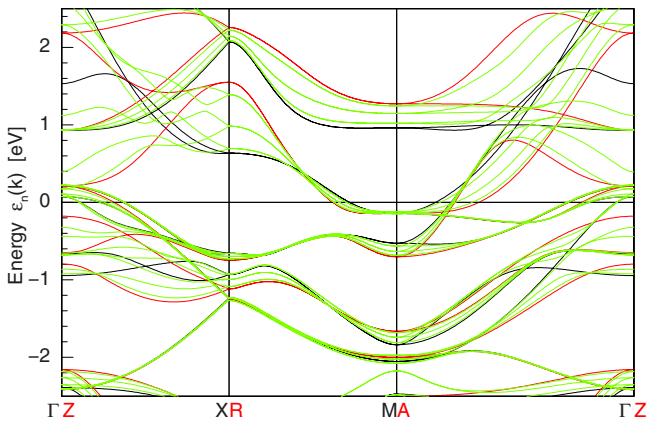

FIG. 3. (Color online) Band plot of bulk LiFeAs for $k_z = 0$ (black) and $k_z = \pi$ (red or dark gray) and slab LiFeAs (green or light gray lines).

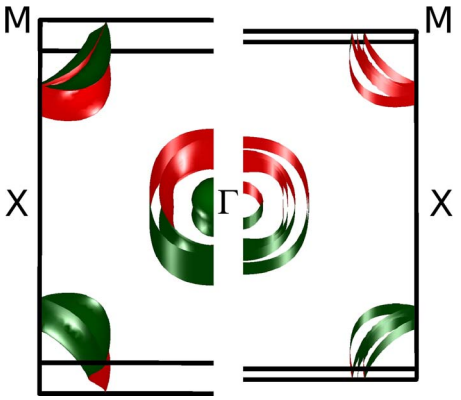

FIG. 4. (Color online) FS of LiFeAs. The Z point is above Γ, the A point above M and, the R point above X. Left panel: bulk. Right panel: slab (no z dispersion; 3D perspective for better visibility only).

Γ-Z-R-A, which couples to As at higher energies and to Fe at lower energies. This effect is absent in all other families of iron pnictides or chalcogenides, i.e., 11 (e.g., FeSe), 1111 (e.g., LaOFeAs), or 122 (e.g., $BaFe_2As_2$).[11] In fact, this dispersive feature is responsible for the closed FS seen around Γ in Fig. 4 (left panel). Of course, in a slab model there is no k_z dispersion and hence this FS is not closed in Fig. 4 (right panel).

As seen in Fig. 3, all slab bands (thin green lines) in the vicinity of the Fermi level are within the k_z-dispersion range of the corresponding bulk bands (pairs of black and red lines). Hence no surface band is found in an energy window free of bulk bands. This is in contrast to the situation found for LaOFeAs in Ref. 1. Furthermore, the bulk FS nesting is less pronounced than in LaOFeAs (larger difference between radii of electron and hole FSs) due to a larger k_z dispersion compared to LaOFeAs, which is mainly caused by the extended Li states. This could be related to the absence of magnetic order in this material.

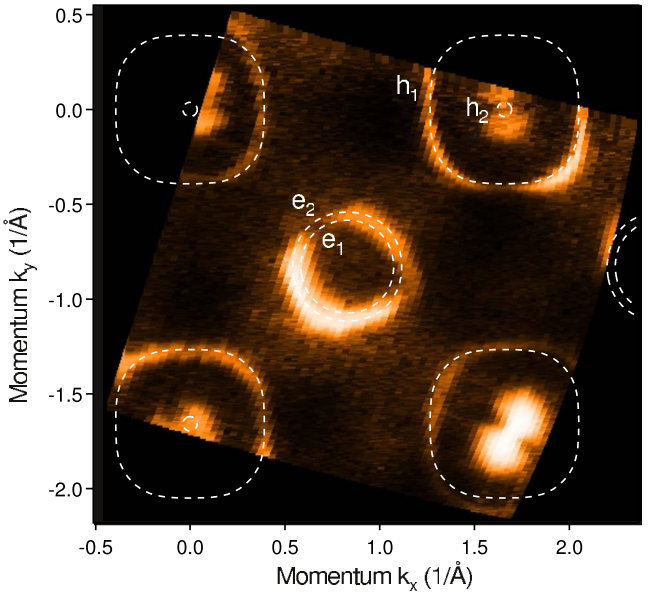

FIG. 5. (Color online) FS of a LiFeAs from angle-resolved photoemission.

TABLE III. Fermi radii in k_x direction of different FS pockets in units of $\frac{2\pi}{a}$ from experimental data and from the calculation.

	M_1	M_2	Γ_1	Γ_2
Experiment	0.15	0.18	0.24	≈0.07
GGA	0.17	0.17	0.19	0.13

We note that Ref. 19 calculated a smaller orbital weight ratio between As $4p$ and Fe $3d$. Although both calculations differ somewhat in the Fe-As layer distance (here 2.345 Å compared to 2.403 Å of Ref. 19) this is mainly caused by different local-orbital projections.

Figure 4 shows the calculated FSs of the bulk and the slab. As can be seen the k_z dependence of the bulk FSs interpolates between the corresponding k_z-dispersionless slab FSs and no indication of surface specific features is found. Hence, surface sensitive experiments will represent the bulk electronic structure.

ARPES results for the FS are shown in Fig. 5. The FS radii are comparable with the calculated results at least in chosen directions while the shape of the FSs around Γ seems to be more complex in experiment. We infer that this finding, just as the band renormalization presented below, is intrinsic to the bulk electronic structure. In Table III the calculated bulk Fermi radii (averaged over k_z) are compared to measured values (see Fig. 5).

In Fig. 6 we compare the experimental ARPES data with the results of the calculations. The spectra were collected at lightsource BESSY, Berlin. A detailed description of the experiment can be found elsewhere (Ref. 15). In the upper panel, we show the photoemission intensity and in the lower panel the corresponding results for the calculated bulk band structure. The photoemission data have been interpolated by a tight binding (TB) fit (denoted by the dotted lines). Note, however, that there are uncertainties in TB fits, especially concerning band connectivities. The holelike structures near the Γ point are indicated by h_1, h_2, and h_3, and electronlike structures near the corner of the BZ by e_1 and e_2. These notations are also used in Fig. 5 (except for h_3, see below).

The energy scale in both panels is of the same width, which allows to estimate the band renormalization. The overall agreement is remarkable, taking into account that in both cases the low-energy electronic structure is formed by five bands and the FS is of the same topology. Applying a renormalization factor to the calculations leads to even better,

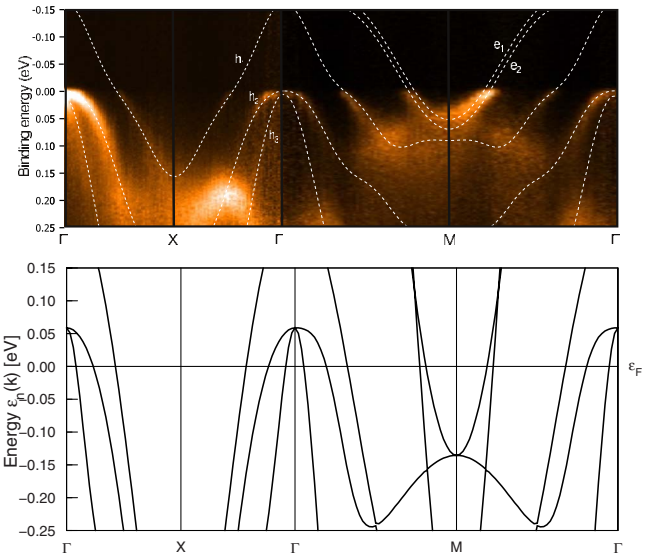

FIG. 6. (Color online) Upper panel: photoemission intensity recorded along the high-symmetry directions in LiFeAs. Lower panel: corresponding results for the calculated bulk band structure.

quantitative agreement. All characteristic dispersions and Fermi velocities are reproduced by the calculations. The experimental Fermi surface (Fig. 5) consists of two holelike FSs around the Γ point and two electronlike FSs centered at the M point. The strongly dispersive h_3 feature (seen in Fig. 6) barely contributes to the spectral weight at the Fermi level and hence is not indicated in Fig. 5. The relative sizes of the Fermi surfaces differ slightly from the theoretical ones. Notably, the first two hole pockets at the zone center seem to be smaller in the ARPES data compared to the calculations. (The agreement can be improved by applying a small shift of the chemical potential. This would also improve the agreement concerning the h_3 feature at the Γ point.)

In summary, we have investigated the surface structure and surface effects on the electronic structure in LiFeAs. The main finding is that due to the neutral cleaving of the compound between the Li layers there are no significant surface effects on the electronic states. Consequently, LiFeAs is an ideal compound in the pnictide family for the study by ARPES and STM methods.

The project was supported, in part, by the DFG under Grants No. KN393/4 and No. BO 1912/2-1 as well as priority program SPP1458.

*h.eschrig@ifw-dresden.de; http://www.ifw-dresden.de/~/helmut

[1] H. Eschrig, A. Lankau, and K. Koepernik, Phys. Rev. B **81**, 155447 (2010).

[2] D. H. Lu, M. Yi, S.-K. Mo, A. S. Erickson, J. Analytis, J.-H. Chu, D. J. Singh, Z. Hussain, T. H. Geballe, R. R. Fisher, and Z.-X. Shen, Nature (London) **455**, 81 (2008).

[3] C. Liu, T. Kondo, A. D. Palczewski, G. D. Samolyuk, Y. Lee, M. E. Tillman, N. Ni, E. D. Mun, R. Gordon, A. F. Santander-Syro, S. L. Bud'ko, J. L. McChesney, E. Rotenberg, A. V. Fedorov, T. Valla, O. Copie, M. A. Tanatar, C. Martin, B. N. Harmon, P. C. Canfield, R. Prozorov, J. Schmalian, and A. Kaminski, Physica C **469**, 491 (2009).

[4] D. H. Lu, M. Yi, S.-K. Mo, J. G. Analytis, J.-H. Chu, A. S. Erickson, D. J. Singh, Z. Hussain, T. H. Geballe, I. R. Fisher, and Z.-X. Shen, Physica C **469**, 452 (2009).

[5] C. Liu, Y. Lee, A. D. Palczewski, J.—Q. Yan, T. Kondo, B. N.

Harmon, R. W. McCallum, T. A. Lograsso, and A. Kaminski, Phys. Rev. B **82**, 075135 (2010).
[6] L. X. Yang, B. P. Xie, Y. Zhang, C. He, Q. Q. Ge, X. F. Wang, X. H. Chen, M. Arita, J. Jiang, K. Shimada, M. Taniguchi, I. Vobornik, G. Rossi, J. P. Hu, D. H. Lu, Z. Y. Shen, Z. Y. Lu, and D. L. Feng, arXiv:1006.1107v1 (unpublished).
[7] H. Liu, G. F. Chen, W. Zhang, L. Zhao, G. Liu, T.—L. Xia, X. Jia, D. Mu, S. Liu, S. He, Y. Peng, J. He, Z. Chen, X. Dong, J. Zhang, G. Wang, Y. Zhu, Z. Xu, C. Chen, and X. J. Zhou, Phys. Rev. Lett. **105**, 027001 (2010).
[8] I. Morozov, A. Boltalin, O. Volkova, A. Vassiliev, O. Kataeva, U. Stockert, M. Abdel-Hafiez, M. Fuchs, H.-J. Grafe, G. Behr, R. Klingeler, S. Borisenko, S. Wurmehl, and B. Büchner, Cryst. Growth Des. **10**(10), 4428 (2010).
[9] Y. J. Song, J. S. Ghim, B. H. Min, Y. S. Kwon, M. H. Jung, and J.—S Rhyee, Appl. Phys. Lett. **96**, 212508 (2010).
[10] J. H. Tapp, Z. Tang, B. Lv, K. Sasmal, B. Lorenz, P. C. W. Chu, and A. M. Guloy, Phys. Rev. B **78**, 060505(R) (2008).
[11] H. Eschrig and K. Koepernik, Phys. Rev. B **80**, 104503 (2009).
[12] T. Miyake, K. Nakamura, R. Arita, and M. Imada, J. Phys. Soc. Jpn. **79**, 044705 (2010).
[13] H. Nakamura, M. Machida, T. Koyama, and N. Hamada, J. Phys. Soc. Jpn. **78**, 123712 (2009).
[14] C. W. Chu, F. Chen, M. Gooch, A. M. Guloy, B. Lorenz, B. Lv, K. Sasmal, Z. J. Tang, J. H. Tapp, and Y. Y. Xue, Physica C **469**, 326 (2009).
[15] S. V. Borisenko, V. B. Zabolotnyy, D. V. Evtushinsky, T. K. Kim, I. V. Morozov, A. N. Yaresko, A. A. Kordyuk, G. Behr, A. Vasiliev, R. Follath, and B. Büchner, Phys. Rev. Lett. **105**, 067002 (2010).
[16] K. Koepernik and H. Eschrig, Phys. Rev. B **59**, 1743 (1999).
[17] J. P. Perdew, K. Burke, and M. Ernzerhof, Phys. Rev. Lett. **77**, 3865 (1996).
[18] M. J. Pitcher, D. R. Parker, P. Adamson, S. J. C. Herkelrath, A. T. Boothroyd, R. M. Ibberson, M. Brunelli, and S. J. Clarke, Chem. Commun. (Cambridge) **2008**, 5918.
[19] D. J. Singh, Phys. Rev. B **78**, 094511 (2008).